Anomalous diffusion in bounded temporally irregular flows

Shankar C. Venkataramani[*]
James Franck Institute,
University of Chicago,Chicago, IL 60637.

Thomas M. Antonsen Jr. and Edward Ott
Department of Physics, Department of Electrical Engineering
and Institute for Plasma Research,
University of Maryland, College Park, MD 20742.

July 8, 1997

Abstract

We investigate the longitudinal dispersion of passive tracers in a transversely bounded shear flow. The flow is assumed to be temporally irregular, but to possess smooth large scale spatial structure without significant small spatial scale motions. We show that, the existence of a region where the longitudinal velocity goes to zero linearly with

[*]E-mail : scvenkat@kam.uchicago.edu

distance from the wall causes the tracers to "stick" to the walls. This results in a *superdiffusive* dispersion of the tracer. We analyze the growth of the variance and show that $\sigma^2(t) \sim t^\nu$ with $\nu = 3/2$. We verify this result by numerical simulation and compare the results from this model with experimental observations.

PACS : 05.45.+b, 47.52.+j, 05.60.+w

Keywords : Anomalous diffusion, Levy Flights, Passive tracer transport, Hamiltonian systems.

1 Introduction

The mixing and transport of a passive tracer by a shear flow is a problem of fundamental interest for a variety of applications in engineering and natural science. In this situation, the interaction between velocity gradients in the flow and mixing of the tracer in the direction transverse to the mean flow leads to longitudinal dispersion of the tracer.

Taylor [1] investigated the longitudinal dispersion of a passive scalar in a steady laminar Poiseuille flow in a pipe. The tracer mixes across the streamlines of the flow by molecular diffusion (with a diffusion coefficient D_m). This allows the tracer to sample the complete profile of the flow. Taylor showed that, for times much longer than $t_0 = a^2/D_m$, [where t_0 is the typical time it takes for a tracer particle to diffuse across the pipe (radius a)], the tracer diffuses in the longitudinal direction with a variance $\sigma^2(t)$ that grows linearly in time. In this case

$$\sigma^2(t) \sim 2\overline{D}t, \tag{1}$$

where $\overline{D} = U^2 t_0/48 = U^2 a^2/(48 D_m)$ is the effective diffusion coefficient and U is the velocity at the center of the pipe.

Some situations show behaviors that differ from the prediction of Eq. (1). In particular, the case where the variance grows as a power law with an exponent not equal to 1,

$$\sigma^2(t) \sim t^\nu, \tag{2}$$

is referred to as *anomalous diffusion*. The case $\nu < 1$ is called *subdiffusive* and the case $\nu > 1$ is called *superdiffusive*. For example, Nordin and Sabol [2] analyze data on the spread of tracers in rivers and find that (2) applies with $\nu \approx 1.4$. Other observations with both passive and active scalars in rivers show anomalous diffusion. For a review of shear dispersion especially in the context of dispersion in rivers, see Young and Jones [3].

Anomalous diffusion has been demonstrated in various fluid flow models and has also been observed in experiments. Young [4] showed that subdiffusive behavior is possible in model flows where the tracer can be "arrested" in stagnant regions of the flow (*e.g.,* in side branches). Subdiffusive behavior is also found in model flows with convective rolls [5] and in experiments with flows where tracers are detained in "sticking regions" (*e.g.* vortices) for long periods of time [6]. Weakly superdiffusive behavior, $\sigma^2(t) \sim t \log t$, has been demonstrated in models of flows through twisted pipes [7, 8]. In these models, the mixing of the tracer in the transverse direction is due to advection by the flow and the tracers tend to be trapped in some regions of the flow leading to the faster than linear growth of variance in these models.

Anomalous diffusion occurs in many different situations, and discussions from the perspective of random walks have been given by Montroll and Shlesinger [9] and Shlesinger *et al.* [10]. Anomalous diffusion occurs in various random walk models that have random walkers which are either in uniform motion or at rest and switch between these two states [11]. If the probability for the random walker to be in uniform motion (a flight) for a time interval of duration t has a power-law tail in t and the mean squared duration of a flight diverges, an ensemble of these random walkers will show superdiffusive behavior. Random walks where the mean square displacement of a single step is infinite are called *Lévy flights.* These models with random walkers undergoing Lévy flights are relevant to transport by advection in fluid flows. In some flows, the tracers can stick to certain regions of the flow like jets or very long-lived vortices, and the above mechanism can lead to superdiffusive transport of the tracer [10].

Power law behavior and anomalous diffusion is also seen in transport in two dimensional (2-D) area preserving maps and Hamiltonian systems [12] - [19]. Karney [12] and Chirikov and Shepelyansky [13] numerically investigate transport in 2-D area preserving maps that have coexisting regular Kolmogorov-Arnold-Moser (KAM) tori and chaotic regions. They observe sticking of chaotic orbits near the KAM boundary between the chaotic and the regular regions, and they find that the probability distribution of the sticking times (time spent near the KAM boundary) has a power law tail. This phenomenon has been investigated analytically by Chirikov [14] using a diffusion model. Meiss and Ott [15] (see also [16]) present a self-similar random walk model based on the successive hierarchical structure of KAM island chains surrounding KAM island chains, and they show how this structure leads to power law time behavior. This power law sticking can lead to anomalous superdiffusive behavior as demonstrated in Refs. [17] - [19]. An incompressible 2-D fluid flow can be described as a Hamiltonian system. Consequently, it is expected that 2-D flows with coexisting regular regions and chaotic regions will lead to anomalous transport of passive tracers as shown in Ref. [19].

The transport of a passive tracer in various fluid flow regimes has been studied experimentally in Refs. [20] - [23]. Fig. 1 is a schematic diagram of the experimental setup. The setup consists of an annular tank that can be rotated. Fluid is pumped into the annular tank through an inner ring of holes (marked I in the figure) and pumped out through an outer ring of holes (marked O) and the setup is then rotated. The velocity field was measured by Solomon *et al.* [24], and they show that the pumping and the rotation sets up an essentially two dimensional flow in the tank. Neutrally buoyant tracers are immersed in the fluid, and their trajectories are tracked by a video camera co-rotating with the speed of the main spatial features of the flow. Depending on the rates of the pumping of the fluid, a variety of flow patterns can be studied including time periodic flows, flows that have an irregular time dependence but exhibit spatially smooth large scale spatial structure, and turbulent flows. (Here we use the word "turbulent" to denote a flow with a complicated time dependence and a velocity field with small scale spatial structure. In contrast, the phrase "temporally irregular" is reserved for flows with a complicated time dependence, but with appreciable spatial variations of the velocity field only on large length scales.)

The video camera is used to track the azimuthal coordinate $\theta(t)$ of the individual tracer particles, and the variance is defined as the spread in the measured angular coordinates of the individual tracers,

$$\sigma^2(t) = \frac{1}{N-1}\sum_{i=1}^{N}(\theta_i(t) - \overline{\theta}(t))^2. \tag{3}$$

In the case of the flow with an irregular time dependence and the case of the time periodic flow, the variance was found to be given by

$$\sigma^2(t) \sim t^{\nu} \tag{4}$$

with $\nu > 1$. In the turbulent case, the diffusion was found to be normal (*i.e.*, $\nu = 1$).

Our study in this paper is motivated by this experiment. In particular, we shall limit our considerations to the regime of the experiment where the velocity field has a time dependence that is temporally irregular but does not exhibit significant small scale spatial structure. Note that, in contrast to the experimental regime where the flow time dependence is periodic, in the case of a temporally irregular flow there can be no KAM surfaces. Thus superdiffusive behavior by the mechanism of power law sticking to KAM surfaces bounding chaotic regions [17]-[19] is not an available explanation for the superdiffusive behavior observed in the temporally irregular regime.

Fig. 2 is an experimentally obtained plot of the variance of the tracer distribution as a function of time on log scales. The inset in Fig. 2 shows the slope of the log-log plot. The existence of a plateau at $\nu = 1.55 \pm 0.25$ for the temporally irregular flow is evidence for anomalous diffusion in this situation. Figs. 3 and 4 show the corresponding plots for a numerical model of this situation that we will discuss later. The numerically obtained plots are qualitatively similar to the experimental plots. Our analysis (discussed in the next section) of the numerical model predicts $\nu = 1.5$ for this situation.

It should be emphasized that the horizontal time scale is logarithmic in the inset of Fig. 2 and in Fig. 4, so that the time interval over which the slope is near 1.5 constitutes most of the measurement time. This can be seen in Fig. 5 which replots the data of Fig. 4 using a linear time scale.

The recent paper of Weeks *et al.* [23] gives a detailed theoretical random-walk-based analysis of the regime where the experimental flow is temporally irregular. To do this, they develop a general Lévy flight random walk model appropriate to their situation. They show that this model is consistent with their experimental results. In doing this they present analysis of experimental data yielding power law flight time and sticking time probability distribution functions. Using the experimentally observed power law exponents in their model, they find agreement with the observed anomalous diffusion exponent [the value of ν in (4)].

Our approach is complementary to that of Ref. [23] in that, we do not base our treatment on a random walk model. Rather, we adopt a model for the flow itself, and we ask how it can yield power law behavior. In particular, we find that a modification of Taylor's model [1] is appropriate. In this new model Taylor's molecular diffusion coefficient D_m is replaced by a space dependent diffusion coefficient which models the transport by the transverse temporally irregular flow. This diffusion coefficient goes to zero as a power of the distance to the wall, and it is this dependence which will lead to superdiffusion. Our work also demonstrates a physical mechanism by which the observed behavior can occur, and makes a definite prediction for the power law exponent for the asymptotic growth of the variance (namely, $\nu = 3/2$). We also analyze our model in terms of the random-walk approach of [23] and compare the predicitons of our model with the exponents measured in experiment [20]-[23].

This approach of adopting a model for the flow gives insight on the dynamical origin of the anomalous exponents for the dispersion. The analysis in this paper should be contrasted with the case of periodic flows which was investigated by Mezić and Wiggins [25]. They show that, in the case of non-ergodic periodic flows, the asymptotic behavior of the variance is $\sigma^2 \sim t^2$, unlike the behavior $\sigma^2 \sim t^{3/2}$ that we find for our model.

2 The model and analysis

We are interested in the situation where the flow velocity is incompressible, has an irregular time dependence but is spatially smooth in that it does not have significant variations on small spatial scales. We consider the situation where the time average flow at each point is longitudinal and the mixing in the transverse direction is entirely due to the temporally irregular variations in the velocity field. We assume that there is an appreciable region near the walls where the longitudinal velocity goes to zero at the wall (no-slip) approximately linearly with distance from the wall. As we will discuss in this section, this causes the tracer to stick to the walls bounding the flow. The probability distribution function of the sticking times of the tracers to the walls has a power law decay such that the expectation of the square of the sticking time diverges. This leads to *Lévy flights* of the tracer particles near the walls and results in the anomalous transport of the tracer. Algebraic decay in the sticking time distributions near a no slip boundary has been investigated in the context of an incompressible Navier-Stokes flow around a cylindrical obstacle in [26].

2.1 Incompressible 2-D flows

Let $\boldsymbol{v} = (v_x, v_y)$ denote a 2-D time dependent incompressible velocity field. Then,

$$\frac{\partial v_x}{\partial x} + \frac{\partial v_y}{\partial y} = 0. \tag{5}$$

This condition is automatically satisfied if the velocities are given in terms of a *stream function* $\psi(x, y, t)$ by

$$\begin{aligned} \dot{x} = v_x &= -\frac{\partial \psi}{\partial y}, \\ \dot{y} = v_y &= \frac{\partial \psi}{\partial x}. \end{aligned} \tag{6}$$

These equations are formally identical to Hamilton's equations for a one degree of freedom system [27] with x being analogous to the momentum, y being analogous to the canonically conjugate coordinate, and the Hamiltonian being analogous to the stream function $\psi(x, y, t)$. If ψ is time-independent, the corresponding Hamiltonian system is integrable since the Hamiltonian is a constant of the motion. Consequently, there are no chaotic trajectories in the phase space. For a 2-D time independent incompressible flow, this implies that a fluid element either has a closed trajectory (it is part of a vortex) or it has an unbounded orbit (a jet). Fig. 6(a) is a schematic representation of the streamlines of a 2-D time independent incompressible flow. In the absence of molecular diffusion, tracers will be trapped on streamlines in such a flow. Consequently, the tracers in a vortex will remain in a vortex indefinitely while the tracers in a jet will be transported ballistically. In this case, the variance asymptotically grows as $\sigma^2(t) \sim t^2$.

If ψ is time dependent, the corresponding Hamiltonian may be non-integrable. If ψ is time-periodic (as for instance in one of the observed regimes of the flow in the rotating annulus experiment), the phase space can consist of coexisting regular regions (jets and vortices) also called KAM regions and chaotic regions. Fig. 6(b) is a schematic representation of this situation. In this case, trajectories in the chaotic region tend to stick to the boundaries of the regular regions for long periods of time. This can lead to anomalous transport of the tracer [19].

If ψ has an irregular time dependence (as for instance in the temporally irregular flow in the rotating annulus experiment), there are no KAM regions in the phase space. This is the situation that we investigate in this paper.

2.2 Sticking to the walls

We consider the situation of a bounded flow where the fluid is between stationary walls at $y = \pm a$. The velocity field satisfies a no-slip boundary condition at $y = \pm a$. Consequently, we have that $v_x = 0$ at $y = \pm a$. Fig. 7 shows the instantaneous longitudinal velocity profile near the boundary at $y = a$. We assume the existence of an appreciable region where the longitudinal velocity goes to zero with distance from the wall *i.e.*,

$$v_x \sim (a - |y|), \tag{7}$$

near $y = \pm a$. Eq. (6) therefore implies that $\psi \sim (a - |y|)^2$ near the boundaries. The velocity field varies over spatial scales of order a, and it is temporally irregular. We then have

$$\psi = f(x,t)(a - |y|)^2 + O((a - |y|)^3), \tag{8}$$

near the boundaries at $y = \pm a$ where $f(x,t)$ is an arbitrary function that is smooth over spatial scales of size a and varies irregularly in time. Equation (6) yields

$$v_y \approx f_x(x,t)(a - |y|)^2, \tag{9}$$

near the walls so that the velocity transverse to the wall goes to zero quadratically near the boundaries. Consequently, a tracer that is close to the wall will remain there for a long period of time. We refer to this as "sticking" to the walls.

At a given position, v_y varies irregularly in time. For time scales longer than the coherence time of the flow, τ_c, a particle near a boundary executes a random walk in the direction transverse to the boundary. Therefore, we can model the transport in the transverse direction close to the boundaries as a diffusion process with a diffusion coefficient given by

$$D = \langle v_y^2 \rangle \tau_c. \tag{10}$$

Using the expression for v_y in (9) we obtain,

$$D(y) \sim (a - |y|)^4. \tag{11}$$

The diffusion model near the wall [i.e., for $(a - |y|)$ small] is justified because the typical step size in a correlation time, $\sqrt{D\tau_c} \sim (a - |y|)^2$, becomes small compared to the distance to the wall, $(a - |y|)$. Thus the transport of tracers in the y direction near the walls at $y = \pm a$ can be modeled as diffusion with a y dependent diffusion coefficient $D(y)$ that approaches zero as the fourth power of distance from the wall, (11).

2.3 Model for tracer transport

The tracer concentration is given by a density $p(x, y, t)$; *i.e.*, $p(x, y, t)$ denotes the number of tracer particles per unit area in a small area element containing (x, y) at time t. [In terms of the experiment of Refs. [20]-[23] (see Fig. 1) we think of x as analogous to the azimuthal coordinate θ, and y as analogous to the radial coordinate.] The transport of tracer is entirely due to the chaotic advection by the flow. Therefore, the tracer flux $\mathbf{\Gamma}$ is given by

$$\mathbf{\Gamma} = p\boldsymbol{v}, \tag{12}$$

where $\boldsymbol{v} = (v_x(x,y,t), v_y(x,y,t))$ is the time dependent flow velocity. The temporally irregular shear flow has a time average longitudinal velocity, $\langle v_x \rangle = v(y)$. Fig. 8 is a schematic representation of the longitudinal velocity profile $v(y)$. There is mixing across the streamlines of this average flow by a temporally irregular velocity field. As discussed in the previous subsection, we can model this mixing in the transverse direction as diffusion in y with a y dependent diffusion coefficient $D(y)$. This is a good model for the transport in this flow near the walls, but it does not accurately reflect the transport of tracer in the interior of the flow (because the step size $\sqrt{D\tau_c} = \langle v_y^2 \rangle^{1/2}\tau_c$ can be $O(a)$ in the central channel region). However, this should not matter for our scaling results because the anomalous transport that we obtain is due to the sticking of the tracers near the walls (we return to this point subsequently). With these considerations, we write the flux $\mathbf{\Gamma}$ as

$$\mathbf{\Gamma} = v(y)p(x,y,t)\hat{\boldsymbol{e}}_x - D(y)\frac{\partial p(x,y,t)}{\partial y}\hat{\boldsymbol{e}}_y. \tag{13}$$

We generalize the expression for $D(y)$ in (11) to consider the class of models that, near the walls, can be described by a y dependent diffusion coefficient of the form

$$D(y) \simeq \tilde{D}\left(\frac{a-|y|}{a}\right)^{\alpha}. \tag{14}$$

The exponent α is four for flows with $v_x \sim (a-|y|)$ and $v_y \sim (a-|y|)^2$. Using the expression for the flux in Eq. (13) in the continuity equation for the density p,

$$\frac{\partial p}{\partial t} + \boldsymbol{\nabla} \cdot \boldsymbol{\Gamma} = 0, \tag{15}$$

we obtain the following diffusion equation,

$$\frac{\partial p}{\partial t} = \frac{\partial}{\partial y}\left[D(y)\frac{\partial p}{\partial y}\right] - v(y)\frac{\partial p}{\partial x}, \tag{16}$$

for the tracer density $p(x, y, t)$. Since the flow is confined by the walls to the region $|y| < a$, we have no-flux in the y-direction as boundary conditions at $y = \pm a$. Consequently,

$$D(y)\frac{\partial p}{\partial y}\bigg|_{y=\pm a} = 0. \tag{17}$$

We also impose the boundary conditions

$$p(x, y, t) \to 0 \qquad \text{as } x \to \pm\infty. \tag{18}$$

Equations (14), (16), (17) and (18) with $\alpha = 4$ constitute our model for the transport of a passive tracer in a bounded shear flow with no-slip at the boundaries.

2.4 Results

Let $E[.]$ denote the expectation over all the tracer particles, *i.e.*,

$$E[h(x, y, t)] = \int_{-a}^{a} dy \int dx\, h(x, y, t)p(x, y, t), \tag{19}$$

where $p(x, y, t)$ is the tracer density. We will define the variance $\sigma^2(t)$ by

$$\sigma^2(t) = E[x^2] - (E[x])^2. \tag{20}$$

We give a complete analysis of the model in Eqs. (16), (17) and (18) and calculate the variance $\sigma^2(t)$ in Appendix A.

For small times, the mixing of the tracers in the transverse direction is negligible. Consequently, the tracers spread ballistically, and initially the variance grows as t^2. We have

$$\sigma^2(t) = \sigma^2(0) + \gamma_0^2 t^2, \tag{21}$$

for $t \ll t_0$ where t_0 is the time scale associated with the transport by the large scale spatial structures in the flow (vortex turnover time) and γ_0^2 is the initial variance in the longitudinal velocity. For $t \gg t_0$, the tracers mix in the transverse direction and their transport is no longer ballistic. We obtain (see Appendix A), $\sigma^2(t) \sim t^\nu$ for large t where

$$\nu = 1 \qquad \text{for } \alpha < 3, \tag{22}$$

and

$$\nu = 2 - \beta \qquad \text{for } \alpha \geq 3, \tag{23}$$

with $\beta = 1/(\alpha - 2)$ (see Appendix A). Therefore, we have normal diffusion of the tracers for $\alpha < 3$ and we have superdiffusive tracer transport for $\alpha > 3$. Fig. 9 is a plot of the asymptotic exponent ν as a function of the exponent α.

We wish to emphasize that these results do not assume any particular form for the transverse velocity profile $v(y)$. The only requirement is that the velocity go to zero as a power law in the distance form the boundary in an appreciable region near the boundary. Thus, we expect that these results should be relevant in describing the dispersion of a passive tracer in a variety of experimental flows that are essentially 2 dimensional, are temporally irregular and are on a bounded domain with the tangential velocity approaching zero near the walls.

3 Numerical simulation

Our diffusion model is good for the transport of tracer near the boundaries. However, in the interior of the flow, the transport is through large scale advection, and diffusion is not a good model for the mixing in the transverse direction. In order to test our predictions for the growth of the variance and the distribution of flight times, we numerically analyze a model fluid flow with the desired gross features.

We consider a model flow where the stream function ψ can be written as the sum of a time independent part ψ_1 and a temporally irregular part ψ_2 We choose ψ_1 to be

$$\psi_1 = -v_0(y - y^3/3), \tag{24}$$

which corresponds to $v_x(x, y) = v_0(1 - y^2)$ and $v_y(x, y) = 0$ for the regular flow. This is a shear flow with no-slip at the boundaries at $y = \pm 1$ (*i.e.*, we take $a = 1$ in this section). The streamlines for this flow are shown in Fig. 10(a). The stream function component ψ_2 for $\alpha = 4$ is chosen to be

$$\psi_2 = \frac{v'}{k_x} \cos(k_x x + \theta(t))(1 - y^2)^2, \tag{25}$$

where $\theta(t)$ varies irregularly in time. Fig. 10(b) shows the instantaneous streamlines of the flow given by ψ_2. This flow models a vortex with a spatial scale $1/k_x$ such that the velocity in the x direction goes to zero as $v_x \sim (1-|y|)$ near the boundaries at $y = \pm 1$. As $\theta(t)$, changes, the vortex pattern moves in the x direction irregularly in time. The coherence time for this flow is the correlation time of $\theta(t)$, and this temporally irregular velocity field is responsible for the mixing of the tracer in the transverse direction.

Although this flow does not capture the exact details of a real experimental flow, it does model the qualitative features of a temporally irregular incompressible flow with the appropriate boundary conditions.

Given the stream function ψ, we can investigate the transport of the tracer by numerically following the trajectories of individual tracer particles. This can be done in a computationally efficient way if we can obtain maps T_n such that

$$T_n : (x, y) \to (x', y'), \tag{26}$$

where (x', y') are the coordinates at time $t = n + 1$ of a fluid element that was at (x, y) at time $t = n$. This scheme is computationally very efficient since we do not have to numerically integrate the trajectories of all the tracer particles. Instead, we apply the map T_n to each tracer particle at time n, repeat using the map T_{n+1} at time $n + 1$, and so on.

The map T_n is generated by an incompressible shear flow with no-slip boundary conditions. Therefore, it is required to have the following properties:

1. The map T_n should be area-preserving.

2. It should have no-slip, *i.e.*, if $y = \pm 1$, $T_n(x, y) = (x, y)$.

We exploit the analogy between 2-D incompressible flows and Hamiltonian systems. Since a Hamiltonian flow generates a *canonical transformation* [28] of the coordinates and the momenta, the map T_n is a canonical transformation. We can generate canonical transformations using the technique of *generating functions* [28]. If $F_n(x', y)$ is an arbitrary function of the coordinate x' at time $n+1$ and the coordinate y at time n, the map $T_n(x,y) \to (x',y')$ defined implicitly by

$$x = \frac{\partial F_n(x',y)}{\partial y}, \qquad y' = \frac{\partial F_n(x',y)}{\partial x'}, \tag{27}$$

is automatically area preserving. Here, x' is implicitly defined in terms of x and y, and we need to invert the equation for x in terms of x' and y to obtain the map T_n. If the continuous time flow is generated by the stream function $\psi(x,y,t)$, the generating function F_n given by

$$F_n = x'y + \psi(x', y, nt_0)t_0, \tag{28}$$

yields a map T_n that is the same to the first order in the time step t_0 as integrating the flow generated by ψ. F_n is a first-order *implicit symplectic integrator* for the flow. (For a discussion of symplectic integration schemes and higher order symplectic integrators, see [29] and references therein).

Imagine integrating the flow (24), (25) using a split step algorithm in which, during the first half of the time step $t_0/2$, we integrate the particle motion due to the regular component ψ_1 [Eq. (24)], and during the second half time step, also of duration $t_0/2$, we integrate the motion arising from the "irregular" component ψ_2 [Eq. (25)]. The action of the temporally irregular flow is given by the following discrete time stream function

$$F_n = x'y + \frac{\rho}{2\pi}\cos(2\pi x' + \theta_n)(1-y^2)^2 \tag{29}$$

with $\theta_n = \theta(nt_0)$ and $\rho = \pi v' t_0/k_x$. This yields a map $Q_n : (x,y) \to (x',y')$ given by

$$\begin{aligned} x &= x' - \frac{2\rho}{\pi}y(1-y^2)\cos[2\pi(x'+r_n)], \\ y' &= y - \rho(1-y^2)^2\sin[2\pi(x'+r_n)], \end{aligned} \tag{30}$$

where $\theta_n = 2\pi r_n$. The action of the longitudinal flow is given by the map

$$P_n : (x_n, y_n) \to (x_n + \lambda(1 - y_n^2), y_n), \tag{31}$$

with $\lambda = v_0 t_0/2$. Composing the maps Q_n and P_n, we obtain the map $T_n : (x_n, y_n) \to (x_{n+1}, y_{n+1})$. It is given by

$$\begin{aligned} x_n &= x_{n+1} - \lambda(1 - y_n^2) - \frac{2\rho}{\pi} y_n(1 - y_n^2)\cos[2\pi(x_{n+1} + r_n)], \\ y_{n+1} &= y_n - \rho(1 - y_n^2)^2 \sin[2\pi(x_{n+1} + r_n)]. \end{aligned} \tag{32}$$

Note that if $y_n = \pm 1$, T_n satisfies the no-slip condition $x_{n+1} = x_n$.

Eqns. (32) constitute the numerical model we use to study the transport of tracer in bounded chaotic shear flows. Since we wish to evolve many particles for a long time, we will be taking rather large time steps. In particular, we set $\lambda = 1$ and choose r_n on each time step to be a random sample uniformly distributed in $[0, 1)$ (with this choice we may think of t_0 as being of the order of the correlation time of the temporally irregular flow). Also, as discussed below, we will choose a value of ρ that is not small. By these choices, we greatly speed the computation, at the expense of not accurately integrating the precise flow given by (24) and (25). This is not really a drawback since, by our construction, the map (32) still represents *some* exactly incompressible flow with no slip boundary conditions. The flow that it represents deviates somewhat from (24) and (25), but, as we discussed earlier, we are only interested in gross features independent of flow details. In particular, we expect that the derived scaling behaviors of the growth of the variance and the distribution of flight times near the walls are universal and are independent of the exact details of the flow. Consequently we endeavor to test our analytic results (21) - (23) for the growth of the variance by numerical simulations using the model flow in (32) with $\lambda = 1$. We invert the equation for x_n in terms of x_{n+1} and y_n using Newton's method. For invertibility, we need that $\rho < 3\sqrt{3}/8 \approx 0.65$. We choose $\rho = 0.3$ for our numerical simulations. We generate r_n at each time step by randomly choosing a sample from $[0, 1)$. We follow 22,000 tracer particles that are initially uniformly distributed in the region $-0.5 < x < 0.5$ and $-1 < y < 1$. The mean position $\overline{x}_n$ is given by

$$\overline{x}_n = \frac{1}{N} \sum_{i=1}^{N} x_n(i), \tag{33}$$

where $x_n(i)$ is the x coordinate of the ith tracer particle at the time step n. The variance of the tracer distribution is then calculated as

$$\sigma_n^2 = \frac{1}{N-1} \sum_{i=1}^{N} (x_n(i) - \overline{x}_n)^2. \tag{34}$$

Fig. 3 is a log-log plot of the variance of the tracer distribution at different time steps. The fitted straight lines have the theoretical slopes of 2 and 3/2 [*c.f.*, Eqs. (21) and (23)]. The numerical data is in good agreement with the analytic predictions. The crossover time t^* between $\sigma^2 \sim t^2$ and $\sigma^2 \sim t^{3/2}$ is given by $t^* \sim 1/\rho^2$, which is the diffusion time scale for the tracers in the central region of the flow.

Fig. 4 is the slope of the log-log plot in Fig. 4. The slope is initially near $\nu = 2$ but then crosses over to a plateau near $\nu = 1.5$ for large times. This is clearly seen in Fig. 5 where the slope of the log-log plot is plotted versus the time step on a linear scale. These plots show good agreement between the analytic prediction for the exponents of the growth of the variance and the results of the numerical simulation.

4 Random Walk models

In this section, we discuss the relation between our model and the asymmetric random-walk models of Weeks *et al.* [23] which also show anomalous diffusion. In the random-walk models relevant to our discussion it is assumed that the particles can be in one of two states [30], in motion with uniform velocity (flights) or at rest (sticking), and there are prescribed probability distributions for the transitions between these states.

The labelling of the states as being stuck and being in flight is an arbitrary choice because changing the frame of reference to a moving frame does not change the variance of the tracer distribution, although taking the frame to move with the original flight state changes the labelling of the states, *i.e,* what is originally the stuck state will now be the flight state and vice versa. In order to avoid this ambiguity, we refer to the two states as State 1 and State 2.

It is assumed that the lifetime distributions in the two states have power law tails with exponents $-\mu_1$ and $-\mu_2$ [31]. The lifetime distribution of a tracer in state 1, $P_1(t)$, is the probability density that the length of time that a tracer spends in state 1 is between t and $t + dt$. It is assumed that, for large t

$$P_1(t) \sim t^{-\mu_1}. \tag{35}$$

Similarly, $P_2(t)$ is the probability density that a random walker is in state 2 for an interval of duration between t and $t + dt$. For large t

$$P_2(t) \sim t^{-\mu_2}. \tag{36}$$

The random walk model is therefore characterized by the exponents μ_1 and

μ_2. If the lifetime distribution in one of the states decays exponentially instead of algebraically, the corresponding exponent is equal to infinity. Weeks *et al.* analyze this model [23] and they determine the anomalous diffusion exponent ν in terms of the exponents μ_1 and μ_2.

4.1 Two state model

Our model for the tracer transport, Eq. (16), has a continuous distribution of longitudinal velocities. In this section, we discuss how this transport process can be analyzed by an equivalent two state model. Let $(x_i(t), y_i(t))$ be the trajectory of the ith tracer particle (in the frame where the walls are at rest). The longitudinal velocity $(v_x)_i(t)$ satisfies $0 \leq (v_x)_i \leq v_0$ for all t.

We generate a two state random walk using following procedure. Choose a time T_0, that is longer than the fast time scale (the vortex turnover time) but is shorter than the length of the experiment. The average longitudinal velocity $u_i(n)$ of the ith tracer in the time interval $nT_0 \leq t < (n+1)T_0$ is given by

$$u_i(n) = \frac{1}{T_0}(x_i((n+1)T_0) - x_i(nT_0)). \tag{37}$$

We choose an arbitrary threshold velocity v_{th} such that $0 < v_{th} < v_0$. Then, a two-state random walk model is defined by putting the ith tracer in state 1 (velocity v_0) for the time interval $nT_0 \leq t < (n+1)T_0$ if $u_i(n) > v_{th}$ and in state 2 (velocity 0) if $u_i(n) \leq v_{th}$.

The trajectories of the tracers defined by the two state random walk depend on the threshold v_{th}. Also, they do not, in general, approximate the real trajectories of the tracers. However, the spreading of the tracers in the real flow is the same as the spreading in the two state model. In particular, the asymptotic exponent for the growth of the variance of the tracers in the actual flow will be found to be the same as for the two-state random walk defined by $u_i(n)$.

The exponents μ_1 and μ_2 are given by the asymptotic distributions of the lifetimes in the states 1 and 2. Since the time step T_0 is an arbitrary parameter, the exponents μ_1 and μ_2 should be independent of the exact value of T_0 for this approximation of the actual trajectory by a two-state random walk model to be valid. The events that correspond to the tracer spending large periods of time in state 2, correspond to the periods of time, where the average longitudinal velocity of a tracer is very small in the frame of reference where the walls are stationary, *i.e,* it corresponds to the events where the tracers are "stuck" near the walls for long periods of time. If the duration of such an event satisfies t is much larger than T_0, the distribution of the durations is independent of the precise value of T_0 that we choose. Since the exponents $\mu_{1,2}$ characterize the long t behavior they are independent of T_0.

We analyze the lifetime distributions for the model in Eq. (16) in Appendix B. We show that the lifetime distribution in state 1 decays exponentially (See Eq. (B-29)) with a decay time of the order of $a^2/\tilde{D}$. Consequently, the exponent $\mu_1 = \infty$. We also show that the lifetime distribution for the events where the tracers remain near the walls (state 2) decays algebraically (See Eq. (B-21) and the exponent $\mu_2 = 2 + 1/(\alpha - 2)$.

We can test these predictions using the numerical model we discuss in Sec. 3 with $\alpha = 4$ (no-slip). We choose $T_0 = 10$ which is bigger than the vortex turnover time ($\sim$ one time step). We choose the threshold velocity $v_{th} = 2/3$, the average velocity of the transverse flow.

Fig. 11 shows a numerically obtained distribution of the lifetimes in state 1. The solid line is a fit. The distribution of lifetimes is exponential with a time constant which is given by the slope of the straight line in the linear-log plot. The value of the slope is consistent with the predicition in the appendix that $\tau \sim a^2/\tilde{D}$. Since the lifetime distribution $P_1(t)$ decays exponentially for large values of t, the exponent $\mu_1 = \infty$.

Fig. 12 shows a numerically obtained distribution of the lifetimes for the events that correspond to the sticking near the walls in the numerical model. We have $\alpha = 4$ (no-slip at the boundary). The distribution of lifetimes is asymptotically a power law. The solid line has the theoretically predicted slope of $-5/2 = -\mu_2$. The agreement between the data and the theoretical predicitions is inconclusive.

From the analysis in Ref. [23], the anomalous diffusion exponent for $\mu_1 = \infty$ and $\mu_2 = 2.5$ is given by

$$\nu = 4 - \mu_2 = 3/2, \tag{38}$$

in agreement with our analysis.

4.2 Random walk models for incompressible flows

The 2-D flow considered in this paper is incompressible. Therefore, the fraction of the tracers in each of the states is asymptotically given by the fraction of the area of the flow that corresponds to each of the two states. In particular, the fraction of the tracers in either of the two states cannot become zero, because the regions of the flow corresponding to each of the two states have finite areas. This requirement constrains the allowed values of the exponents μ_1 and μ_2 for incompressible 2-D flows.

Let $p_1(t)$ and $p_2(t)$ denote the fraction of the tracers in state 1 and state 2 at time t. Then, by an analysis of this situation similar to the analysis in Ref. [23], we can show that,

1. If $\mu_1 > 2$ and $\mu_2 > 2$, the mean lifetimes in the states 1 and 2 are finite and are given by

$$\langle t_j \rangle = \int_0^\infty t P_j(t)\, dt \qquad j = 1, 2. \tag{39}$$

   In that case,

$$E[p_1(t \to \infty)] = \langle t_1 \rangle / (\langle t_1 \rangle + \langle t_2 \rangle), \tag{40}$$

   and similarly for $E[p_2(t)]$. In this situation, both the fractions are non-zero asymptotically.

2. If $\mu_1 < 2 < \mu_2$, the mean lifetime in state 1 is infinite but the mean lifetime in state 2 is finite. In this case, we have

$$E[p_2(t)] \sim t^{-(2-\mu_1)}. \tag{41}$$

   This situtation is not possible in an incompressible flow as it will lead to all the particles eventually ending up in state 1. Similarly, $\mu_2 < 2 < \mu_1$ is also ruled out.

3. If $\mu_1 \leq \mu_2 \leq 2$, the mean lifetimes in both states are infinite. However, the fraction of the tracer in state 2 is given by

$$E[p_2(t)] \sim t^{-(\mu_2-\mu_1)}. \tag{42}$$

   If we want that $E[p_2(t)]$ remain finite as $t \to \infty$, it is neccessary that $\mu_1 = \mu_2$.

Consequently, for a two state random walk approximation of a 2D flow, incompressibility implies that either

$$\mu_1 > 2 \qquad \text{and} \qquad \mu_2 > 2 \qquad\qquad \text{or} \qquad \mu_1 = \mu_2 \leq 2. \tag{43}$$

The mean flow velocity for a two state random walk model is

$$\overline{v} = E[v_1 p_1(t \to \infty) + v_2 p_2(t \to \infty)].$$

Since both states have nonzero area in an incompressible flow, the value of the mean flow velocity $\overline{v}$ will be intermediate between v_1 and v_2, the velocities of the two states. In particular, the average velocity will not be zero in a frame comoving with one of the states, *i.e.*, where one of the states has a zero velocity. Consequently, for an incompressible flow, the mean position of the tracers $\langle x \rangle$ will scale as

$$\langle x \rangle \approx \overline{v} t, \tag{44}$$

with

$$v_2 < \overline{v} < v_1, \tag{45}$$

where we assume $v_1 > v_2$. Our results that either $\mu_1 > 2, \mu_2 > 2$ or $\mu_1 = \mu_2 \leq 2$ for an incompressible flow are the same as the constraints that can be derived from the results for the scaling of the mean position that are obtained in [23] by imposing the requirement that Eqs. (44) and (45) be satisfied.

4.3 Rotating annulus experiment

Weeks *et al.* analyze the rotating annulus experiment [23] using the two state random walk model. By looking at the tracer trajectories, they can clearly distinguish the times when the particle is "stuck" in a vortex and the times when the particle is in "flight" motion relative to the vortices. In our nomenculature, we identify their "flights" with state 2 and their "stickings" with state 1.

Results for tracer dynamics in temporally irregular flow have been reported for two different experimental conditions. In particular, the temporally irregular flows described in Refs. [21, 22] involved angularly inhomogenous pumping in which the inflow/outflow through the holes in the tank bottom (see Fig. 1) was blocked in a 60^o sector of the tank. Reference [23], on the other hand utilized angularly homogenous pumping (with different parameters from Refs. [21, 22]). For the case of Refs. [21, 22], analysis of the experimental data yields a value of the anomalous diffusion exponent [22] of $\nu = 1.55 \pm 0.25$ in good agreement with our theoretical result of $\nu = 3/2$. Their experimental exponent for state 2 (motion near the walls) [22] is $\mu_2 \approx 2.6$ in agreement with our theoretical result $\mu_2 = 5/2$. For state 1, our theoretical model has exponential decay of $P_1(t)$. In Ref. [22] they comment that $P_1(t)$ is "perhaps power law at intermediate times with crossover to exponential behavior at longer times but the data are inconclusive." At any rate, there is no contradicition to our prediction of exponential decay for $P_1(t)$ ($\mu_1 = \infty$). Thus we obtain fairly good agreement between the theory and the data of Refs. [21, 22]. The data of Ref. [23] presents a somewhat more problematic situation. The increase of the variance is "clearly superdiffusive with an exponent between 1.5 and 2.0." The authours, however, also comment on the "failure of the variance to reach its asymptotic behavior" during the time of the experiment. the state 2 distribution shows [23] a clear power law decay, $P_2(t) \sim t^{-\mu_2}$ with $\mu_2 = 1.9 \pm 0.2$ in disagreement with our theoretical result of $\mu_2 = 5/2$ with $\alpha = 4$. According to Eq. (B-21), a value of μ_2 approaching 2 results as α becomes very large in our theory. A large value of α corresponds to a flow for which v_y approaches zero very rapidly as one approaches the wall (See Eqs. (14) and (10).) For the behavior of $P_1(t)$, "the behavior is sometimes unclear. In some cases it appears that there is a crossover to exponential decay at very long times."

5 Conclusions

In this paper we study the longitudinal dispersion of a passive scalar in a bounded temporally irregular shear flow with no KAM surfaces. The tracer tends to stick to the walls because of the no slip boundary conditions on the flow. This results in anomalous diffusion of the tracer and the variance asymptotically grows with an exponent of 3/2. We also verify this result by numerical simulation. This study was motivated by experimentally observed anomalous diffusion in 2-D incompressible temporally irregular flows. We propose a model that incorporates the effects of the boundarry conditions of the flow and provides a possible physical mechanism for the observed algebraic decays and Lévy flights in fluid flows.

Acknowledgement

We would like to thank Eric Weeks and Harry Swinney for useful discussions and for providing us with a prepublication copy of their paper, Ref. [23]. This research was supported by the Office of Naval Research. The numerical computations reported in this paper were made possible by a grant from the W. M. Keck foundation.

Appendices

Appendix A Growth of variance

We will analyze Eq. (16) with the boundary conditions (17) and (18) using the moments of the distribution of the tracer. We define the nth moment, M_n, by

$$M_n(t) = \int_{-a}^{a} dy \int_{-\infty}^{\infty} dx\, x^n p(x, y, t). \tag{A-1}$$

The tracer is initially distributed in a bounded region in x, so that $p(x, y, 0) = 0$ for $|x| \geq X_0$. Since the tracer is advected by a flow with a bounded longitudinal velocity with $|v(y)| \leq v_0$, we have that $p(x, y, t) = 0$ for $|x| \geq X_0 + v_0 t$. Consequently, all the moments $M_n(t)$ are well defined for all times t. The variance $\sigma^2(t)$ is given by

$$\sigma^2(t) = M_2(t) - (M_1(t))^2 \tag{A-2}$$

We also define the linear density of the nth moment, $\mu_n(y, t)$, by

$$\mu_n(y, t) = \int_{-\infty}^{\infty} dx\, x^n p(x, y, t). \tag{A-3}$$

Multiplying Eq. (16) by x^n and integrating over x, we obtain

$$\frac{\partial \mu_n}{\partial t} = \frac{\partial}{\partial y}\left[D(y)\frac{\partial \mu_n}{\partial y}\right] + nv(y)\mu_{n-1}, \tag{A-4}$$

where we use the fact that $p(x, y, t) = 0$ for $|x| \geq X_0 + v_0 t$. Integrating these equations over y we obtain the equation

$$\frac{\partial M_n}{\partial t} = \int_{-a}^{a} dy\, nv(y)\mu_{n-1}(y, t), \tag{A-5}$$

which governs the evolution of the moments M_n.

In order to solve for the long time behavior of the variance, we Laplace transform (A-4) to obtain

$$s\overline{\mu}_n(y;s) - \mu_n(y,0) = \frac{d}{dy}\left[D(y)\frac{d\overline{\mu}_n(y;s)}{dy}\right] + nv(y)\overline{\mu}_{n-1}(y;s), \qquad \text{(A-6)}$$

where $\overline{\mu}_n(y;s)$ is the Laplace transform of $\mu_n(y,t)$. $\overline{\mu}_n(y;s)$ satisfies a no-flux boundary condition

$$D(y)\frac{d\overline{\mu}_n(y;s)}{dy} = 0 \qquad \text{at } y = \pm a. \qquad \text{(A-7)}$$

We now consider the case $v(y) = v(-y)$ for $0 \le y \le a$ and $D(y) = D(-y) = (a - |y|)^\alpha$. Then if $p(x,y,0)$ is symmetric about $y = 0$, $\mu_n(y,t)$ is symmetric about $y = 0$ for all t. This will enable us to restrict our attention to the region $0 \le y \le a$ so that both $D(y)$ and $v(y)$ are smooth functions of y and have derivatives to all orders except at $y = a$. The symmetry implies that we can now solve for $\overline{\mu}_n(y;s)$ with the boundary conditions

$$D(y)\frac{d\overline{\mu}_n(y;s)}{dy} = 0 \qquad \text{at } y = a, \qquad \text{(A-8)}$$

and

$$\frac{d\overline{\mu}_n(y;s)}{dy} = 0 \qquad \text{at } y = 0. \qquad \text{(A-9)}$$

We define $z = a - y$. This leads us to consider the homogenous problems,

$$sw_i - \frac{d}{dz}\left[z^\alpha \frac{dw_i}{dz}\right] = 0 \qquad i = 1, 2, \qquad \text{(A-10)}$$

with w_1 satisfying the boundary condition

$$z^\alpha \frac{dw_1}{dz}\bigg|_{z=0} = 0, \qquad \text{(A-11)}$$

and w_2 satisfying the boundary condition

$$\left.\frac{dw_2}{dz}\right|_{z=a} = 0. \tag{A-12}$$

We use w_1 and w_2 to construct a *Green's function* for the original problem. We want the behavior of the solution for long times, *i.e.*, for small s. We can expand w_2 in powers of s for $z \neq 0$ as

$$w_2 = g_0 + sg_1 + s^2 g_2 + \ldots, \tag{A-13}$$

where

$$\begin{aligned} g_0(z) &= 1, \\ g_1(z) &= \frac{z^{2-\alpha}}{2-\alpha} - \frac{az^{1-\alpha}}{1-\alpha}, \end{aligned} \tag{A-14}$$

and so on. We must proceed differently to obtain an approximation to w_1. In particular, because $z^\alpha \to 0$ as $z \to 0$, we can not treat s as a small parameter and expand w_1 in the form

$$w_1 = f_0 + sf_1 + s^2 f_2 + \ldots. \tag{A-15}$$

Instead we first scale s out of the equation by defining $u = zs^{-\beta}$, where $\beta = 1/(\alpha - 2)$ as defined earlier. With this rescaling, we have

$$\frac{d}{du} u^\alpha \frac{dw_1}{du} = 0, \tag{A-16}$$

with the boundary condition

$$\left. u^\alpha \frac{dw_1}{du}\right|_{u=0} = 0. \tag{A-17}$$

Let ϕ_1 and ϕ_2 be the two linearly independent solutions of (A-16). For $u \gg 1$, the two independent solutions are

$$\phi_1(u) = 1 + \frac{u^{2-\alpha}}{2-\alpha} + \ldots, \tag{A-18}$$

and

$$\phi_2(u) = u^{1-\alpha} + \frac{u^{3-2\alpha}}{(3-2\alpha)(2-\alpha)} + \ldots. \tag{A-19}$$

In order to satisfy the boundary condition at $u = 0$, we will have

$$w_1(z) = \phi_1(zs^{-\beta}) + c\phi_2(zs^{-\beta}), \tag{A-20}$$

where c is a nonzero constant. Therefore, we have

$$w_1(z) = 1 + cs^{1-\beta}y^{1-\alpha} + \frac{sy^{2-\alpha}}{2-\alpha} + \ldots \tag{A-21}$$

for $zs^{-\beta} \gg 1$. We can calculate the Wronskian $W = w_1 w_2' - w_2 w_1'$ at a point z such that $z \gg s^\beta$ and we get

$$W(z) = -asz^{-\alpha}\left[1 + c_1 s^\beta + c_2 s + \ldots\right], \tag{A-22}$$

so that $z^\alpha W(z)$ is independent of z as we expect. The constants c_1 and c_2 are independent of z and s but depend on a. The Green's function with these boundary conditions is given by

$$G(z, z'; s) = \frac{-w_1(z^<)w_2(z^>)}{z_0^\alpha W(z_0)}, \tag{A-23}$$

where $z^< = \min(z, z')$ and $z^> = \max(z, z')$. The product $z_0^\alpha W(z_0)$ is independent of the point z_0 that is chosen. We now have

$$G(z, z'; s) = \frac{1}{as}\left[1 + \Phi_1(z, z')s^\beta + \Phi_2(z, z')s + \ldots\right], \tag{A-24}$$

where the functions Φ_1 and Φ_2 are determined by expanding the Green's function in powers of s. We can now drop the symmetry restriction on v and the restriction that $D(y) = (a - |y|)^\alpha$. All we require is that near $y = \pm a$,

$D(y) \to 0$ with an exponent α. In this general case, we can write down the solution to (A-6) as

$$\overline{\mu}_n(y;s) = \int_{-a}^{a} dy'\, G(y,y';s) \left[\mu_n(y',0) + nv(y)\overline{\mu}_{n-1}(y';s)\right], \tag{A-25}$$

where by analogy with the symmetric case, the Green's function is given by

$$G(y,y';s) = \frac{G_0}{s}\left[1 + \Psi_1(y,y')s^{\beta} + \Psi_2(y,y')s + \ldots\right], \tag{A-26}$$

and the functions $\Psi_1, \Psi_2, \ldots$ determine an expansion of G in powers of s. If $v(y) = \overline{v}_x$ is a constant independent of y and the initial distribution of the tracers is uniform along $x = 0$ *i.e.*,

$$p(x,y,0) = \frac{1}{2a}\delta(x), \tag{A-27}$$

the distribution of the tracers at a time t is given by

$$p(x,y,t) = \frac{1}{2a}\delta(x - \overline{v}_x t). \tag{A-28}$$

In this case, $\mu_0(y,t) = 1/(2a)$ for all t. Therefore, $\overline{\mu}_0(y;s) = 1/(2as)$. Using Eq. (A-25) for μ_0, we obtain,

$$\begin{aligned} G_0 &= \frac{1}{2a}, \\ \int_{-a}^{a} \Psi_i(y,y')dy' &= 0 \qquad \text{for all } i. \end{aligned} \tag{A-29}$$

Therefore, we have

$$G(y,y';s) = \frac{1}{2as} + \tilde{G}(y,y';s), \tag{A-30}$$

where

$$\tilde{G}(y,y';s) = \frac{1}{2as}\left[\Psi_1(y,y')s^{\beta} + \Psi_2(y,y')s + \ldots\right], \tag{A-31}$$

satisfies

$$\int_{-a}^{a} \tilde{G}(y, y'; s)dy = \int_{-a}^{a} \tilde{G}(y, y'; s)dy' = 0. \tag{A-32}$$

Let $i_n(y)$ denote the inital condition $\mu_n(y, 0)$. Then $\overline{\mu}_n(y; s)$, the Laplace transform of the density of the nth moment, is given by Eq. (A-25) as

$$\overline{\mu}_n(y, s) = \int_{-a}^{a} G(y, y'; s)i_n(y')dy' + \int_{-a}^{a} G(y, y'; s)v(y')\overline{\mu}_{n-1}(y', s)dy'. \tag{A-33}$$

The Laplace transforms of the moments, $\overline{M}_n$, are given by

$$\overline{M}_n = \int_{-a}^{a} \overline{\mu}_n(y, s)dy. \tag{A-34}$$

and Eq. (A-5) for the evolution of the moments can be written as

$$\overline{M}_n = \frac{2a}{s} \left[\langle i_n(y)\rangle + \langle v(y)\overline{\mu}_{n-1}(y, s)\rangle\right], \tag{A-35}$$

where we use the notation $\langle f(y)\rangle$ to denote the average value of a function $f(y)$ over the interval $-a \leq y \leq a$, *i.e.*,

$$\langle f\rangle = \frac{1}{2a} \int_{-a}^{a} f(y)dy. \tag{A-36}$$

We can use this equation along with the Eq. (A-25) for the densities $\overline{\mu}_n$ and Eq. (A-26) for the Green's function to determine the behavior of the moments M_1 and M_2, from which we can determine the asymptotic growth of the variance $\sigma^2(t)$.

We have a freedom to choose the frame of reference for our analysis of the variance. We will choose the frame which is moving with respect to the stationary walls at the average velocity of the flow. We can write the time averaged longitudinal velocity in the frame where the walls are stationary as $v(y) = \overline{v}_x + \tilde{v}(y)$ where $\overline{v}_x = \langle v(y)\rangle$ is the average longitudinal velocity, Then, the velocity in the moving frame is $\tilde{v}(y)$ and $\langle \tilde{v}(y) \rangle = 0$. In the moving frame, the the tracer density $p'(x', y', t')$ is given by

$$p'(x', y', t') = p(x' + \overline{v}_x t, y', t'), \tag{A-37}$$

and it satisfies the equation

$$\frac{\partial p'}{\partial t'} = \frac{\partial}{\partial y'} \left[D(y) \frac{\partial p'}{\partial y'} \right] - \tilde{v}(y') \frac{\partial p'}{\partial x'}. \tag{A-38}$$

This equation is the same as Eq. (16) with $v(y)$ replaced by $\tilde{v}(y)$. Therefore, by our earlier result Eq. (A-25), we have

$$\overline{\mu}'_0(y, s) = \frac{\langle i_0 \rangle}{s} + \int_{-a}^{a} \tilde{G}(y, y'; s) i_0(y') dy'. \tag{A-39}$$

Using $\langle \tilde{v}(y) \rangle = 0$, Eq. (A-35) yields

$$\overline{M}'_1(s) = \frac{2a}{s} \left[\langle i_1 \rangle + \frac{1}{2a} \int_{-a}^{a} \int_{-a}^{a} \tilde{v}(y) \tilde{G}(y, y'; s) i_0(y') dy' dy \right], \tag{A-40}$$

The expression for $\overline{\mu}'_0(y, s)$ in Eq. (A-39) along with Eq. (A-33) yields,

$$\begin{aligned} \overline{\mu}'_1(y, s) \;\; = \;\; & \frac{\langle i_1 \rangle}{s} + \int_{-a}^{a} \tilde{G}(y, y'; s) i_1(y') dy' \\ & + \frac{1}{2as} \int_{-a}^{a} \int_{-a}^{a} \tilde{v}(y') \tilde{G}(y', y''; s) i_0(y'') dy' dy'' \\ & + \frac{\langle i_0 \rangle}{s} \int_{-a}^{a} \tilde{G}(y, y'; s) \tilde{v}(y') dy' \\ & + \int_{-a}^{a} \int_{-a}^{a} \tilde{G}(y, y'; s) \tilde{v}(y') \tilde{G}(y', y''; s) i_0(y'') dy' dy''. \end{aligned} \tag{A-41}$$

We can now determine the second moment M'_2 in the moving frame of reference using Eq. (A-35). We obtain

$$\overline{M}'_2 \;\; = \;\; \frac{2a}{s} \left[\langle i_2 \rangle + \frac{1}{a} \int_{-a}^{a} \int_{-a}^{a} \tilde{v}(y) \tilde{G}(y, y'; s) i_1(y') dy' dy \right.$$

$$
+\frac{\langle i_0\rangle}{as}\int_{-a}^{a}\int_{-a}^{a}\tilde{v}(y')\tilde{G}(y',y'';s)\tilde{v}(y'')dy'dy''
$$
$$
+\frac{1}{2a}\int_{-a}^{a}\int_{-a}^{a}\int_{-a}^{a}\tilde{v}(y)\tilde{G}(y,y';s)\tilde{v}(y')\tilde{G}(y',y'';s)i_0(y'')dy''dy'dy.\Big] \tag{A-42}
$$

We use the expansion for $\tilde{G}(y,y';s)$ for small s as in Eq. (A-31). For $\beta<1$, *i.e.*, $\alpha>\alpha_{crit}=3$, we get the following asymptotic forms for $M_1'(t)$ and $M_2'(t)$. We have

$$
\begin{aligned}
M_1'(t) &= \frac{1}{2a}\frac{t^{1-\beta}}{\Gamma(2-\beta)}\int_{-a}^{a}\int_{-a}^{a}\tilde{v}(y)\Psi_1(y,y')i_0(y')dydy' \\
M_2'(t) &= \left(\frac{\langle i_0\rangle}{2a}\right)\frac{2t^{2-\beta}}{\Gamma(3-\beta)}\int_{-a}^{a}\int_{-a}^{a}\tilde{v}(y)\Psi_1(y,y')v(y')dydy' \qquad \text{(A-43)}
\end{aligned}
$$

Consequently, $\sigma^2(t)=M_2(t)-M_1^2(t)$ implies that asymptotically we have $\sigma^2(t)\sim t^{2-\beta}$.

If $\beta>1$, we then have the following asymptotic forms for M_1' and M_2', *viz.*,

$$
\begin{aligned}
M_1'(t) &= \frac{1}{2a}\int_{-a}^{a}\int_{-a}^{a}\tilde{v}(y)\Psi_2(y,y')i_0(y')dydy' \\
M_2'(t) &= 2t\left(\frac{\langle i_0\rangle}{2a}\right)\int_{-a}^{a}\int_{-a}^{a}\tilde{v}(y)\Psi_2(y,y')v(y')dydy' \qquad \text{(A-44)}
\end{aligned}
$$

In this case, $\sigma^2(t)\sim t$. These equations give the exponents for the asymptotic growth of the variance. The results are summarized in Fig. 9.

Appendix B Waiting times

The distribution of times where the moving average of the longitudinal velocity is less than a threshold is denoted by $P_2(t)$. The time-scale over which the velocity is averaged is denoted by T_0. We choose the threshold velocity as $v_{th} = v(a - \Delta)$. Then, for $\Delta \ll a$, a event where the ith tracer particle is in state 2 will roughly correspond to an event where a tracer is within a distance of order Δ from the boundary because the time scales for diffusing out of this region are much longer than T_0. In a time T_0, a tracer will diffuse in y by an amount $y_{diff} \sim (D(a-\Delta)T_0)^{1/2} = (\tilde{D}T_0)^{1/2}(\Delta/a)^{\alpha}$, which is much smaller than Δ for $\Delta \ll a$. Consequently, for $t \gg T_0$ the probability density that this event has a length between t and $t + dt$ is roughly the same as the probability density that a tracer remains within a distance Δ from the boundary for a time between t and $t + dt$.

We will consider the sticking of a tracer near the boundary at $y = a$, *i.e.*, is in state 2. Similar considerations also apply to sticking near $y = -a$ and it suffices to consider the boundary near $y = a$ to derive the lifetime distribution. Let $\rho_2(t)$ denote the total amount of tracer that stays within the distance Δ of the boundary at $y = a$ until a time t. $\rho_2(t)$ is given by

$$\rho_2(t) = \int_{a-\Delta}^{a} dy \int dx\, \hat{p}(x, y, t) \tag{B-1}$$

where $\hat{p}(x, y, t)$ is a solution to the equation

$$\frac{\partial \hat{p}}{\partial t} = \frac{\partial}{\partial y}\left[D(y)\frac{\partial \hat{p}}{\partial y}\right] - v(y)\frac{\partial \hat{p}}{\partial x}, \tag{B-2}$$

with an initial condition that is the tracer density at the beginning of a event when the tracer is in state 2, a no-flux boundary condition

$$D(y)\frac{\partial \hat{p}}{\partial y} = 0, \tag{B-3}$$

at $y = a$ and an absorbing boundary condition

$$\hat{p}(x, y, t) = 0, \tag{B-4}$$

at $y = a - \Delta$.

We impose the absorbing boundary condition at $y = a - \Delta$ since, once a particle leaves the region within a distance Δ of the wall, we regard it as being in state 1. This is an approximation. However, as we discuss earlier, if the averaging time T_0 is small compared to the diffusion times in the region $y \sim a - \Delta$, this approximation is valid because the distances that a tracer diffuses through in a time T_0 is of the order of $y_{diff} \ll \Delta$. Therefore, the tracers that are in state 2 are almost all entirely in the region $a - \Delta < y < a$ and tracers outside this region are in state 1. We also have the boundary conditions $\hat{p}(x, y, t) \to 0$ as $x \to \pm\infty$.

Because these boundary conditions are different from the one which is applied to Eq. (16) [*viz.* Eqs. (17) and (18)] , we distinguish the present density $\hat{p}$ from p the solution of Eq. (16) and its boundary conditions Eqs. (17) and (18). We define the linear density of the tracer (also see Appendix A)

$$\hat{\mu}_0(y, t) = \int dx \, \hat{p}(x, y, t). \tag{B-5}$$

Integrating Eq. (B-2) over x we obtain,

$$\frac{\partial \hat{\mu}_0}{\partial t} = \frac{\partial}{\partial y} \left[D(y) \frac{\partial \hat{\mu}_0}{\partial y} \right], \tag{B-6}$$

with no-flux at $y = a$ and absorbing boundary conditions at $y = a - \Delta$. The expression for $D(y)$ in (14) is good near the wall and the proportionality constant $\tilde{D}$ is of the order of $D(y = 0)$.

We first analyze the problem where the tracers are initially uniformly distributed in the region $a - \Delta < y < a$. Therefore, we impose the initial condition $\hat{\mu}(y, 0) = 1/\Delta$ for $a - \Delta < y < a$. [Eq. (B-6) with a dependence $D(y) \sim y^\alpha$ is also considered by Chirikov [14] as a diffusive model for sticking to a one-dimensional KAM boundary (y= 0).] Analytic solution of the stated problem is not possible. However, the important time asymptotic properties of the solution can be determined from the self similar solution [14]

$$\hat{\mu}_0(y,t) = \mu_0 H(u), \tag{B-7}$$

where, close to the wall at $y = a$, the scaled variable u is given by

$$u = \left(\frac{a-y}{a}\right)\left[\frac{\tilde{D}}{a^2}(t+\tilde{t})\right]^{\beta}, \tag{B-8}$$

with $\beta = 1/(\alpha - 2)$. $H(u)$ satisfies

$$\frac{d}{du}\left[u^{\alpha} H'(u)\right] = \beta u H'(u), \tag{B-9}$$

where

$$H(u) = \int_{\infty}^{u} H'(u)du, \tag{B-10}$$

so that $H(u) \to 0$ as $u \to \infty$, which is an absorbing boundary at $u = \infty$. We can solve (B-9) to get

$$H'(u) = Cu^{-\alpha}\exp(-1/u^{\alpha-2}). \tag{B-11}$$

We normalize H so that $H(0) = 1$. Thus

$$H(u) = \frac{\int_u^{\infty} u^{-\alpha}\exp(-1/u^{\alpha-2})\,du}{\int_0^{\infty} u^{-\alpha}\exp(-1/u^{\alpha-2})\,du}. \tag{B-12}$$

In this case, $H(u) \approx 1$ for $u \ll 1$ and $H(u) \approx 0$ for $u \gg 1$. Fig. 13 is a schematic plot of $H(u)$ that reflects the features of the solution.

In the definition of u we choose the constant $\tilde{t}$ so that $u = 1$ at $t = 0$ and $a = y - \Delta$. Therefore,

$$\tilde{t} = \left(\frac{a}{\Delta}\right)^{\alpha}\frac{\Delta^2}{\tilde{D}}. \tag{B-13}$$

This choice of $\tilde{t}$ yields an initial condition which roughly approximates that desired for $\hat{\mu}_0(y,0)$. Although the self-similar solution (B-7) does not satisfy the absorbing boundary condition at $y = a - \Delta$ at a finite time, as $t \to \infty$, $\hat{\mu}_0(a-\Delta, t) \to \mu_0 H(\infty) = 0$. Therefore, the self-similar solution is the asymptotic solution to the diffusion equation (B-2) with an absorbing boundary at $y = a - \Delta$.

To determine the distribution of the lifetimes in state 2, we need to solve Eq. (B-2) with boundary conditions (B-3) and (B-4) but with the initial condition $\hat{p}(x,y,0) = \delta(x)\tilde{\mu}_0(y)$ where $\tilde{\mu}_0(y)$ represents the distribution of tracers at the start of the event. Consequently, $\tilde{\mu}_0(y)$ has a support $y \in [a-\Delta, a-\Delta+y_{diff}]$. We assume that the initial condition is a uniform density on this set. Then, the initial condition is the difference between two step functions, one with support $[a-\Delta, a]$ and the other with support $[a, a-\Delta+y_{diff}]$. Therefore, the initial condition can be written as

$$\tilde{\mu}_0(y,0) \approx H[u(t=0)] - H[u'(t=0)], \tag{B-14}$$

where u is the scaling variable defined in Eq. (B-8) and u' is a similar scaling variable with Δ replaced by $\Delta - y_{diff}$, so that

$$u' = \left(\frac{a-y}{a}\right)\left[\frac{\tilde{D}}{a^2}(t+\tilde{t}')\right]^{\beta}, \tag{B-15}$$

with

$$\tilde{t}' = \left(\frac{a}{\Delta - y_{diff}}\right)^{\alpha}\frac{(\Delta - y_{diff})^2}{\tilde{D}}. \tag{B-16}$$

Since Eq. (B-6) is a linear time-invariant equation and the boundary conditions are also linear and time independent, the solution of Eq. (B-6) with the initial conditions appropriate to the distribution of tracers at the beginning of an event is given by

$$\tilde{\mu}_0(y,t) \approx H(u) - H(u'), \tag{B-17}$$

and the error in the approximation goes to zero asymptotically.

Therefore, $\rho_2(t)$, the total amount of tracer that stays within a distance Δ of the boundary for a time t is given by

$$\rho_2(t) = \int_{a-\Delta}^{a} \tilde{\mu}_0(y,t)\, dy \sim (t+\tilde{t})^{-\beta} - (t+\tilde{t}')^{-\beta}. \tag{B-18}$$

Consequently, for $t \gg \tilde{t}$, we obtain

$$\rho_2(t) \sim t^{-(1+\beta)} \tag{B-19}$$

The lifetime distribution $P_2(t)$ is the probability density that a tracer is in state 2 for a time between t and $t+dt$. Therefore,

$$P_2(t) = -\frac{d\rho_2(t)}{dt} \sim t^{-(2+\beta)}. \tag{B-20}$$

Consequently, the exponent μ_2 is given by

$$\mu_2 = 2 + 1/(\alpha - 2) = 2 + \beta. \tag{B-21}$$

We now determine $P_1(t)$, the lifetime distribution in state 1. By the argument at the beginning of this section, if $t \gg T_0$ and the diffusion length $y_{diff} \ll \Delta$, the lifetime distribution in state 1 is given by the probability density that a tracer particle that switches from state 2 to state 1 remains in the region $|y| < a - \Delta$ for a time between t and $t+dt$.

The total amount of tracer that stays in the region $|y| < a - \Delta$ is $\rho_1(t)$. Then,

$$\rho_2(t) = \int_{-(a-\Delta)}^{(a-\Delta)} dy \tilde{\mu}_0(y,t) \tag{B-22}$$

where $\tilde{\mu}_0(y,t)$ is a solution to the equation

$$\frac{\partial \tilde{\mu}}{\partial t} = \frac{\partial}{\partial y}\left[D(y)\frac{\partial \tilde{\mu}_0}{\partial y}\right], \tag{B-23}$$

with an initial condition that is the tracer density at the beginning of an event where the tracer is in state 1, and an absorbing boundary condition

$$\tilde{\mu}_0(y,t) = 0, \tag{B-24}$$

at $y = \pm(a-\Delta)$. The absorbing boundary conditions ensure that an event ends when a tracer leaves the region $|y| < a - \Delta$. The initial condition for the solution of interest is the density of the tracers at the beginning of an event. Therefore, the initial condition is roughly a uniform density on the set $[-(a-\delta), -(a-\delta)+y_{diff}] \cup [(a-\delta)-y_{diff}, (a-\delta)]$. For our model, we have, for $|y| \leq a - \Delta$,

$$0 < D(a-\Delta) \leq D(y) \leq D_{max} < \infty, \tag{B-25}$$

so that $D(y)$ is bounded below and above by positive non-zero quantities. Therefore, the diffusion operator in Eq. (B-23) is non-singular and we can solve the eigenvalue problem

$$\frac{\partial}{\partial y}\left[D(y)\frac{\partial \phi(y)}{\partial y}\right] + \lambda\phi(y) = 0, \tag{B-26}$$

with the absorbing boundary conditions at $y = \pm(a-\Delta)$. Because the differential operator is nonsingular, it will have a discrete spectrum of eigenvalues. Let λ_0 denote the smallest positive value for which Eq. (B-26) has a solution satisfying the boundary conditions and let $\phi_0(y)$ be the corresponding solution. Then $\phi_0(y)$ is zero only at $|y| = a - \Delta$ as it can't have any nodes.

Also, if λ_1 is the next smallest eigenvalue, because the spectrum is discrete, $\lambda_1 - \lambda_0 > 0$ and for sufficiently large t, $Ae^{-\lambda_1 t}/Be^{-\lambda_0 t}$ can be made arbitrarily small for arbitrary constants A and B. Consequently, in the long time limit, we can write the solution for $\tilde{\mu}(y,t)$ as

$$\tilde{\mu}(y,t) \sim \phi_0(y)e^{-\lambda_0 t}. \tag{B-27}$$

Asymptotically, we have

$$\rho_1(t) \sim e^{-\lambda_0 t}, \tag{B-28}$$

and

$$P_1(t) = -\frac{d\rho_1(t)}{dt} \sim e^{-\lambda_0 t}. \tag{B-29}$$

Consequently, the lifetime distribution for state 1 decays exponentially with a decay time $\tau = 1/\lambda_0$. From the bounds on $D(y)$, we have $a^2/D(a-\Delta) \leq \tau \leq a^2/D_{max}$. The exponential decay of the lifetime distribution implies that the exponent $\mu_1 = \infty$.

References

[1] G. I .Taylor, R. Soc. London Ser. A **219**, 186 (1953).

[2] C. F. Nordin and G. V. Sabol, Water Resour. Inves. **20-74**, 332 pp. (1974).

[3] W. R. Young and S. Jones, Phys. Fluids A **3**, 1087 (1991).

[4] W. R. Young, J. Fluid Mech. **193**, 129 (1988).

[5] W. Young, A. Pumir and Y. Pomeau, Phys. Fluids A **1**, 462 (1989).

[6] O. Cardoso and P. Tabeling, Eur. J. Mech. B/Fluids **8**, 459 (1989).

[7] S. W. Jones and W. R. Young, J. Fluid Mech. **280**, 149 (1994).

[8] S. W. Jones, Physica D **76**, 55 (1994).

[9] E. W. Montroll and M. F. Shlesinger, in *Nonequilibrium Phenomena II*, edited by J. L. Lebowitz and E. W. Montroll (Elsevier, Amsterdam 1984).

[10] M. F. Shlesinger, G. M. Zaslavsky and J. Klafter, Nature **263**, 31 (1993).

[11] G. Zumofen and J. Klafter, Phys. Rev. E**47**, 851 (1993).

[12] C. F. F. Karney, Physica D **8**, 360 (1983).

[13] B. V. Chirikov and D. L. Shepelyanski, Physica D **13**, 394 (1984).

[14] B. V. Chirikov in *Dynamical Systems and Chaos : Proceedings of the Sitges Conference on Statistical Mechanics*, edited by H. Araki, J. Ehlers, K. Hepp, R. Kippenhahn, H. A. Weidenmüller and J. Zittartz (Springer-Verlag, Berlin, 1983) .

[15] J. D. Meiss and E. Ott, Phys. Rev. Lett. **55**, 2741 (1985);
J. D. Meiss and E. Ott, Physica D **20**, 387 (1986).

[16] J. D. Hansen, J. R. Cary and J. D. Meiss, J. Stat. Phys. **39** 27 (1985).

[17] T. Geisel, A. Zacherl and G. Radons, Phys. Rev. Lett. **59**, 2503 (1987).

[18] R. Ishizaki, H. Hata, T. Horita and H. Mori, Prog. Theor. Phys. **84**, 179 (1990).

[19] A. A. Chernikov, R. Z. Sagdeev and G. M. Zaslavsky, in *Topological Fluid Mechanics*, edited by H. K. Moffat and A. Tsinober (Cambridge University Press, Cambridge, 1990) p.45.

[20] T. H. Solomon, E. R. Weeks and H. L. Swinney, Physica D, **76**, 70 (1994).

[21] T. H. Solomon, E. R. Weeks and H. L. Swinney, Phys. Rev. Lett. **71**, 3975 (1993).

[22] E. R. Weeks, T. H. Solomon, J. S. Urbach and H. L. Swinney, in *Levy flights and Related topics in Physics*, edited by M. F. Shlesinger, G. M. Zaslavsky and U. Frisch (Springer-Verlag, Heidelberg, 1995).

[23] E. R. Weeks, J. S. Urbach and H. L. Swinney, Physica D **97**, 291 (1996).

[24] T. H. Solomon, W. J. Holloway and H. L. Swinney, Phys. Fluids, **5**, 1971 (1993).

[25] I. Mezić and S. Wiggins, Phys. Fluids, **6**, 2227 (1994).

[26] C. Jung, T. Tel and E. Ziemniak, Chaos, **3**, 555 (1993);
E. M. Ziemniak, C. Jung and T. Tel, Physica D **76**, 123 (1994).

[27] H. Aref, J. Fluid Mech. **143**, 1 (1984).

[28] H. Goldstein, *Classical Mechanics*, Addison-Wesley, New York, 1965.

[29] E. Forest and R. D. Ruth, Physica D **43**, 105 (1990);
H. Yoshida, Physics Lett. A **150**, 262 (1990).

[30] Weeks *et al*, consider a three state random walk model with sticking and flights in both directions. The two state model can be obtained by taking an extreme case of the three state model where the probability of getting into one of the flights states (say the flights to the left) is zero.

[31] Weeks *et al*, call the flight exponent μ and the sticking exponent ν. We use μ_1 and μ_2 to avoid confusion with the anomalous diffusion exponent ν.

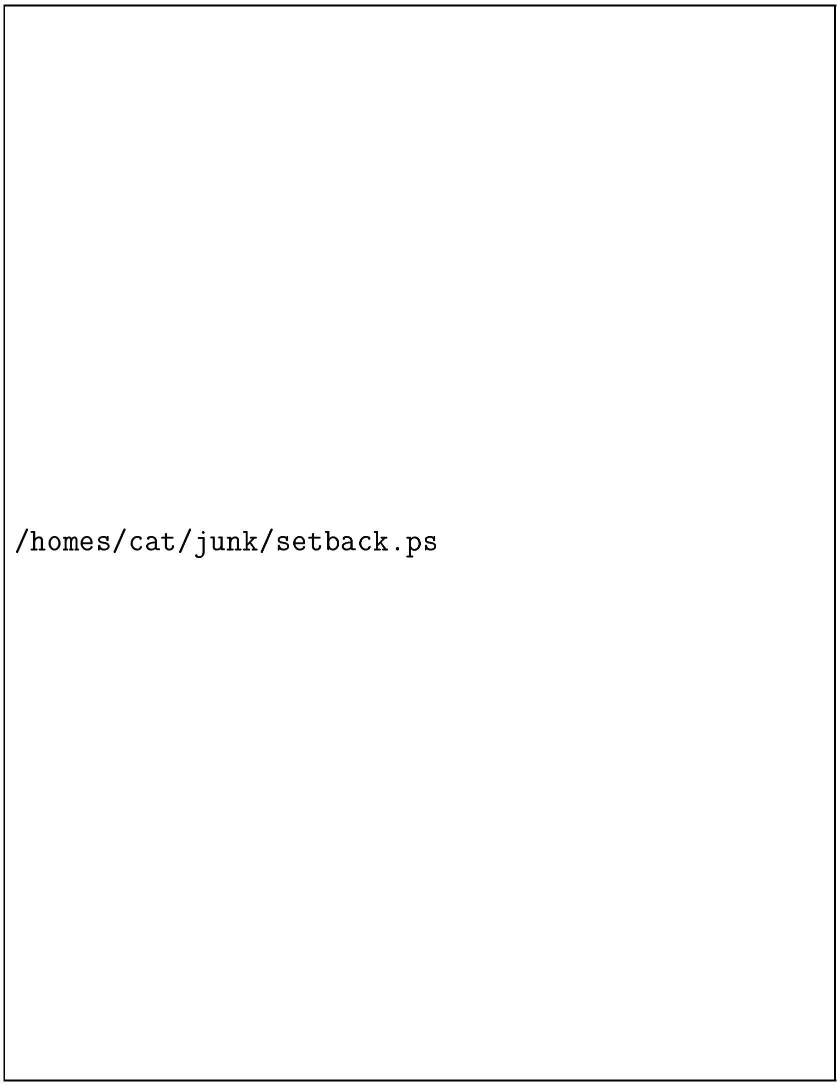

Figure 1: The setup for the rotating annulus experiment. This figure is reprinted from T. H. Solomon, E. R. Weeks and H. L. Swinney, Physica D, **76**, 70 (1994).

Figure 2: Experimentally obtained plot of the variance of the tracer distribution. This plot is reprinted from T. H. Solomon, E. R. Weeks and H. L. Swinney, Physica D, **76**, 70 (1994).

/homes/cat/idl/var.ps

Figure 3: The variance of the tracer distribution for the numerical flow in Sec. 3.

/homes/cat/idl/slp.ps

Figure 4: The slope of the growth of the tracer variance.

/homes/cat/idl/slp_lin.ps

Figure 5: The exponent for the growth of the variance on a linear time scale.

/homes/cat/junk/kam.ps

Figure 6: Stroboscopic surface of section map for (a) The time independent flow and (b) The time periodic flow.

/homes/cat/junk/noslp.ps

Figure 7: The longitudinal velocity near the boundary at $y = a$.

/homes/cat/junk/profil.ps

Figure 8: Profile of the time-averaged longitudinal velocity.

/homes/cat/idl/nuvsbe.ps

Figure 9: The exponent for the asymptotic growth of the variance.

/homes/cat/junk/vrtx.ps

Figure 10: The streamlines for the model flow. (a) The streamlines of the regular flow. The flow velocity is zero at the walls. (b) The streamlines of the temporally irregular flow at an instant of time. The pattern moves around as $\theta(t)$ changes.

/homes/cat/junk/flt.ps

Figure 11: The distribution of lifetimes when the tracers are not stuck to the walls. The solid line is a fit.

/homes/cat/junk/stk.ps

Figure 12: The distribution of lifetimes in state 2. The solid line has the theoretical slope of -5/2.

../junk/pltg.ps

Figure 13: A plot of the self-similar solution $H(u)$. The dashed lines correspond to the scaled location of the absorbing boundary at $y = a - \Delta$ at three different instants of time $t_1 < t_2 < t_3$. As $t \to \infty$, the absorbing boundary moves to large u and the solution asymptotically satisfies the boundary condition at $y = a - \Delta$.